Autonomic Nervous System Activity Measured Directly and QT Interval Variability in Normal and Pacing-Induced Tachycardia Heart Failure Dogs

Gianfranco Piccirillo, MD, PhD[*,‡], **Damiano Magrì, MD**[†], **Masahiro Ogawa, MD, PhD**[‡], **Juan Song, PhD**[†], **Voon J. Chong**[‡], **Seongwook Han, MD, PhD**[‡], **Boyoung Joung, MD, PhD**[‡], **Eue-Keun Choi, MD, PhD**[‡], **Samuel Hwang, BS**[‡], **Lan S. Chen, MD**[§], **Shien-Fong Lin, PhD**[‡], and **Peng-Sheng Chen, MD**[‡]

[*] Dipartimento di Scienze dell'Invecchiamento, Università degli Studi di Roma "La Sapienza," Rome, Italy

[†] U.O.C. Cardiologia, Ospedale S. Andrea, Università degli Studi di Roma "La Sapienza," Rome, Italy

[‡] Krannert Institute of Cardiology, Department of Medicine, Indiana University School of Medicine, Indianapolis, Indiana

[§] Department of Neurology, Indiana University School of Medicine, Indianapolis, Indiana

Abstract

Objectives—This study sought to find out more about the relationship between sympathetic and vagal nerve activity and the cardiac repolarization in a canine model of pacing-induced tachycardia congestive heart failure (CHF).

Background—The QT variability index (QTVI), a noninvasive marker of temporal cardiac repolarization dispersion, is among the risk factors for sudden death during CHF. Among factors influencing this variable are the myocardial damage and the autonomic nervous system activity typical of dilated cardiomyopathy.

Methods—We assessed autonomic nervous system activity recorded from an implanted data transmitter that monitored integrated left stellate-ganglion nervous activity, integrated vagus nerve activity, and electrocardiogram. We collected 36 segments recorded at baseline and 36 after induced CHF. We then arbitrarily identified recording segments as containing low or high sympathetic activity values, and we compared corrected QT intervals and the QTVI under a given sympathetic activity condition at baseline and after inducing CHF.

Results—In the high sympathetic activity subgroup, both QT variables increased from baseline to CHF (corrected QT intervals, $p < 0.01$; QTVI, $p < 0.05$) whereas in the low sympathetic activity subgroup they remained unchanged. The baseline QTVI correlated inversely with integrated vagus nerve activity ($r^2 = 0.16$; $\beta = -0.47$; $p < 0.05$) whereas, during CHF, the QTVI correlated directly with integrated left stellate-ganglion nervous activity ($r^2 = 0.32$; $\beta = 0.27$, $p < 0.01$).

Conclusions—During CHF, sympathetic activation is associated with an increase in the QT interval and QTVI. Because these changes vary over time, they could result from myocardial structural damage and sympathetic activation combined. Conversely, under normal conditions, no relationship exists between sympathetic activation and the QT variables.

Reprint requests and correspondence: Dr. Gianfranco Piccirillo, Dipartimento di Scienze dell'Invecchiamento, I Clinica Medica, Policlinico Umberto I, Viale del Policlinico, 00161 Rome, Italy. gianfranco.piccirillo@uniroma1.it.

Keywords

autonomic nervous system; QT variability index; congestive heart failure; sudden cardiac death

Congestive heart failure (CHF) due to post-ischemic dilated cardiomyopathy is now among the major known risk factors for sudden cardiac death (SCD). Though the complex mechanisms underlying this phenomenon remain partly unclear, accumulating evidence suggests a major role of the autonomic nervous system (ANS). According to the multifactorial mechanism proposed by Zipes and Wellens (1), a sudden increase in sympathetic activity along with diminished vagal nerve activity could act singly or in concert as transient events triggering malignant ventricular arrhythmias culminating in SCD (1). Chronic neurohumoral activation probably prepares the anatomic-functional CHF substrate (1) by inducing myocardial ion channel dysfunction (2,3) thereby prolonging myocardial repolarization and increasing its temporal dispersion. These electrophysiological changes are indirectly assessed with the QT variability index (QTVI), a noninvasive measure of myocardial repolarization lability that is typically increased in CHF (4–6) and correlates closely with an increased risk of SCD (7–9).

Notwithstanding the recent reports questioning the QTVI-ANS relationship (10) and criticizing automated template methods for calculating the QT (11), given that the ANS can alter RR interval variability then it could logically also alter QTVI (see formula in Methods section). Previous studies have investigated these relationships with beta-blockers and maneuvers for stimulating sympathetic nerve activity in healthy subjects and patients with CHF (5,6). Our group recently introduced an invasive technique for directly measuring left stellate ganglion nerve activity (SGNA), vagal nerve activity (VNA), and electrocardiogram (ECG) in ambulatory dogs (12,13). Using this technique, in a previous study others in our research group have already provided evidence that in dogs with CHF experimentally induced with an elaborate protocol (including atrioventricular block, myocardial infarction, and infusion of nerve growth factor), stimulation delivered to the left SGN prolongs the QT, the T-peak to T-end interval, and induces tachycardia or ventricular fibrillation (14). What is now lacking is direct evidence documenting the relationship between the ANS and temporal myocardial repolarization dispersion during nonpharmacologically induced CHF.

To find out more about the relationships between the ANS and temporal myocardial repolarization dispersion during CHF, we designed this experimental study using the canine model of tachycardia pacing-induced CHF to investigate how the ANS influences the QTVI (12). To clarify the influence of RR intervals on cardiac repolarization, we analyzed QT-RR interval cross-spectral coherence.

Methods

Surgical preparation and electrical recording

The data analyzed came from a previous study conducted in 6 female dogs (12). The surgical procedures and the temporal relationship between cardiac arrhythmia and ANS activity are reported in detail elsewhere (12,15). In brief, a high-frequency pacing lead was implanted in the right ventricular apex and connected to an Itrel neurostimulator (Medtronic, Minneapolis, Minnesota) in a subcutaneous pocket. We then implanted a Data Sciences International (DSI) D70-EEE transmitter (St. Paul, Minnesota) with 3 bipolar recording channels for simultaneous recording of SGNA, VNA from the left thoracic vagal nerve located above the aortic arch, and subcutaneous ECG. After implantation, the Itrel stimulator was initially turned off for 2 weeks to allow the dogs to recover from surgery and to allow us obtain baseline recordings. The stimulator was then programmed to pace at 150 beats/min for 3 days, at 200 beats/min for 3 days, and then at 250 beats/min for 3 weeks to induce CHF. The pacemaker was then turned

off to allow an additional 2 weeks of ambulatory monitoring and recording during CHF. All CHF data were recorded within the first week. All dogs underwent echocardiography and venous blood sampling to determine serum N-terminal brain natriuretic peptide concentrations at baseline and after rapid pacing. The animal experiments were approved by the Institutional Animal Care and Use Committee.

Direct measurement of autonomic nervous activity

Data were recorded real time at a sampling rate of 1,000 samples per second per channel, then analyzed offline. The custom-designed software used has been described elsewhere (12,15). In brief, to analyze long-term trends in the large segmented data files effectively, a custom-designed program was developed using Labview software to automatically import, filter, and analyze the DSI transmitter data for ANS activities and heart rates. The software determined the activation cycle lengths (RR intervals) automatically derived from ECG, based on a Hilbert transform algorithm (16). Integrated data from the stellate ganglion (iSGNA) and vagal nerve (iVNA) were high-pass (200 Hz) filtered and rectified over a fixed time segment (Figs. 1 and 2). Because RR intervals shorter than 200 ms were usually due either to ectopic beats, artifacts, or rhythm disturbances, they were removed and excluded from analysis.

To assess ANS activity in greater detail, we selected ECG recording epochs lasting 300 s and containing known iSGNA values (300 s iSGNA) and classified them into 2 subgroups, 1 containing low and the other high sympathetic activity levels, defined according to whether the mean iSGNA value for the segment was over or below an arbitrary value of 80 mV (50th percentile). A further 2 measures were calculated for integrated nerve activities: iSGNA and iVNA over 24 h (24 h iSGNA and 24 h iVNA).

QT variability and QT-RR coherence

To calculate the QT interval and make the end of the T-wave easier to identify, we used a software program based upon the algorithm for quantifying beat-to-beat fluctuations in QT interval variability proposed by Berger et al. (4) and previously validated.

To obtain the QTVI from the 256-beat segments recorded, we calculated QT and RR mean (QT_m and RR_m) and variances (QT_v and RR_v) (Figs. 3 and 4). The QTVI was then determined with the following formula: $QTVI = \log_{10}\{[(QT_v)/(QT_m)^2]/[(RR_v)/(RR_m)^2]\}$. The digitalized ECG recordings were analyzed by a single physician (G.P.).

The same 256-beat segments of ECG were analyzed with autoregressive power spectral (17) and cross-spectral analysis (Fig. 3) (4,5). The next variable estimated was the coherence function for the RR and QT intervals. Coherence expresses the fraction of power at a given frequency in either time series and is explained as a linear transformation of the other, thus providing an index of a linear association between the 2 signals (4,5). The coherence function $\gamma(f)$ was then computed according to the formula:

$$\gamma(f) = \frac{|P_{xy}(f)|^2}{P_{xx}(f)P_{yy}(f)}$$

where f is frequency, $P_{xx}(f)$ is the spectrum of an RR interval, $P_{yy}(f)$ is the QT interval spectrum, and $P_{xy}(f)$ is the cross spectrum. The coherence function provides a measure between zero and unity of the degree of linear interaction between RR and QT interval oscillations as a function of their frequency. Mean coherences were measured by averaging $\gamma(f)$ over the frequency bands: from 0 to 0.50 Hz (Fig. 4).

The QT interval was measured over 256 consecutive beats and corrected for heart rate. The following QT interval corrections (QTc) were applied: (QTc_{Bazett}: $QT/RR^{0.5}$), Fridericia ($QTc_{Fridericia}$: $QT/RR^{0.33}$), Tabo (QTc_{Tabo}: $QT/RR^{0.3879}$), Van de Water ($QTc_{Van\ de\ Water}$: $QT -0.087\ [RR -1]$) (18), and Framingham ($QTc_{Framingham}$: $QT +0.154\ [1 - RR]$).

Data and statistical analysis

For each dog, 6 recordings were obtained at baseline and 6 after pacing-induced CHF, 3 recordings at low sympathetic activity and 3 at high sympathetic activity values according to iSGNA values. A total of 72 recordings were therefore analyzed, 36 obtained at baseline and 36 during CHF. A single rater (J.S.) randomly identified for each dog 6 recordings during CHF, each lasting 5 min, having a good quality ECG trace, and then analyzed the corresponding sympathetic activity recordings. The rater then identified for each dog 6 baseline recordings having similar sympathetic activity and the corresponding 5-min ECG recordings. At baseline and during CHF, the total number of ECG recordings was divided into 2 groups using iSGNA values of 80 mV (50th percentile) as a cutoff. This procedure yielded 4 groups: baseline low sympathetic activity (<50th percentile of iSGNA); baseline high sympathetic activity (<50th percentile of iSGNA); CHF low sympathetic activity (<50th percentile of iSGNA); and CHF high sympathetic activity (<50th percentile of iSGNA). For the statistical comparison between the various groups, the variables obtained from the 5-min ECG recordings from the same dog were randomly paired.

Unless otherwise indicated, all data are expressed as mean ± SD. Data with skewed distribution are given as median and interquartile range (75th to 25th percentile). Paired *t* test was used to compare data for the normally distributed variables (including RR_m, QT_m, QTc, QTVI, QT-$RR_{coherence}$, 300 s iSGNA, and iVNA). Wilcoxon signed rank test was used to compare non-normally distributed variables (including QT_v and RR_v) measured before and after pacing-induced CHF and in the same dog subgroups (low or high sympathetic activity). Corrections were not made for the use of multiple correlated observations within each animal in each condition.

Because an increase in the variables evaluating cardiac repolarization (QT_m, QT_v, QTc_{Bazett}, $QTc_{Fridericia}$, QTc_{Tabo}, $QTc_{Van\ de\ Water}$, $QTc_{Framingham}$, QTVI) indicates an unfavorable event, we assessed for each variable during cardiac repolarization differences between low and high sympathetic activity recordings during CHF, and differences in high sympathetic activity between baseline and CHF recordings. Increased QTVI values were considered a "positive" response and decreased QTVI a "negative" response. A McNemar test was therefore used to substantiate that baseline data and pacing-induced changes in low sympathetic activity and high sympathetic activity recordings differed statistically.

To assess the influence of the ANS on the studied variables at baseline and during pacing-induced CHF, we used stepwise multiple regression analysis, again using as independent variables natural logarithm (ln) iSGNA and ln iVNA, and as single dependent variables the others (RR_m, RR_v, QT_m, QT_v, QTc_{Bazett}, $QTc_{Fridericia}$, QTc_{Tabo}, $QTc_{Van\ de\ Water}$, $QTc_{Framingham}$, and QTVI). All data were evaluated with the database SPSS-PC+ (SPSS-PC+ Inc., Chicago, Illinois). A p value of ≤0.05 was considered statistically significant.

Results

After pacing-induced CHF, in all 6 ambulatory dogs studied the left ventricular ejection fraction decreased significantly from baseline (from 56 ± 4% to 27 ± 7%, p < 0.0001). N-terminal brain natriuretic peptide baseline levels increased (from <180 to 273 pmol/l at baseline, 558 to more than 3,000 pmol/l on CHF day 1, and 405.7 ± 167 pmol/l [273 to 687 pmol/l] on CHF day 14 [p < 0.05]).

As expected, at baseline and after pacing-induced CHF, iSGNA values were significantly higher in high sympathetic activity than in low sympathetic activity recordings (Table 1), whereas no difference was found between iVNA values in the 2 subgroups. In all dogs, 24-h iSGNA and 24-h iVNA values increased during the course of CHF (24-h iSGNA at baseline 143 ± 28 vs. during CHF 186 ± 95, $p < 0.001$; 24-h iVNA at baseline 3 ± 1 vs. 24-h during CHF 8 ± 5, $p < 0.001$).

At baseline, RR_m was significantly longer in low sympathetic activity than in high sympathetic activity recordings ($p < 0.05$) (Table 1), whereas during pacing-induced CHF no difference was found between the subgroups. Last, during CHF, RR_v was significantly lower than at baseline regardless of sympathetic activity levels ($p < 0.05$) (Table 1).

At baseline, QT_m was significantly longer in the low sympathetic activity than in high sympathetic activity recordings ($p < 0.001$) (Table 1). Conversely, during pacing-induced CHF, QT_m was significantly longer in the sub-group recorded at high than at low sympathetic activity levels (Table 1). QT_m in segments recorded at high sympathetic activity levels was significantly shorter at baseline than during pacing-induced CHF ($p < 0.001$) (Table 1). At baseline, QT_v overlapped in the 2 subgroups. Conversely, after pacing-induced CHF, QT_v was significantly lower in low sympathetic activity than in high sympathetic activity recordings ($p < 0.001$) (Table 1).

All of the corrected QT interval values (QTc_{Bazett}, $QTc_{Fridericia}$, QTc_{Tabo}, $QTc_{Van de Water}$, and $QTc_{Framingham}$) measured in the subgroup with high sympathetic activity levels were significantly higher during pacing-induced CHF than at baseline ($p < 0.01$) (Table 1). During CHF, all these corrected QT values were higher in low sympathetic activity than in high sympathetic activity recordings ($p < 0.01$).

During pacing-induced CHF, QTVI values were significantly higher in segments recorded at high sympathetic activity levels than in those at low levels (-2.63 ± 0.50 vs. -2.20 ± 0.26, $p < 0.01$), and at high sympathetic levels were also significantly higher during CHF than at baseline ($p < 0.05$) (Fig. 5). At baseline, no difference was found between QTVI values in segments recorded at low and high sympathetic activity levels (-2.51 ± 0.38 vs. -2.57 ± 0.66, $p = 0.796$) (Fig. 5).

At baseline, mean coherence was significantly greater in segments recorded at high than at low sympathetic activity levels (0.661 ± -0.1330 vs. 0.550 ± -0.139, $p < 0.05$) (Fig. 6) whereas no significant difference was found in this variable between the 2 sympathetic activity subgroups during CHF (low sympathetic activity 0.575 ± 0.153 vs. high sympathetic activity 0.589 ± 0.187, $p = 0.814$) (Fig. 6). Of the 18 comparisons between QTVI values recorded at low and high sympathetic activity levels during CHF, in 15 comparisons QTVI values increased (chi-square 6.7, $p = 0.008$). In the 3 comparisons in which QTVI decreased, the recordings came from 3 different dogs. The other QT-related variables showed a similar pattern of changes: in 17 of the 18 comparisons QTv increased (chi-square 12.5, $p < 0.0001$), and in all 18 comparisons corrected QT values were higher in high sympathetic activity than in low sympathetic activity recordings (chi-square 16.0, $p < 0.0001$). In the comparison between the 2 conditions baseline versus CHF, both recorded at high sympathetic levels, in all 18 comparisons QTVI and all the other QT variables studied increased (chi-square 16.0, $p < 0.0001$).

The stepwise multiple regression analysis testing data recorded at baseline detected a significant positive relation between iVNA and RR interval duration, RRv and all QTcs (Table 2). Under the same condition, the QTVI also correlated negatively with iVNA (Table 2). Conversely, the regression analysis testing data recorded after pacing-induced CHF detected a significant positive relationship between iSGNA and QTv, all QTcs, and QTVI (Table 3).

Discussion

In this study using pacing-induced CHF in ambulatory dogs, as well as confirming the relationship between the ANS and temporal myocardial repolarization dispersion as assessed by the QTVI, we provide new, direct evidence showing an association between sympathetic activity and the QTVI, at least during CHF. The clinical importance of this research finding resides in the knowledge that an increased QTVI is related to an increased risk of sudden death (7–9). We achieved these results thanks mainly to the novel experimental approach that enabled us to assess ANS activity and myocardial repolarization in ambulatory dogs uninfluenced by pharmacological treatment or other confounding factors.

QT, QTVI, ANS, and pathophysiological implications

Our findings show that even though vagal modulation in normal conditions lengthens the RR interval and QT interval this change is balanced by the increased RR_v and by the constant QT_v, thus reducing the QTVI (Table 2). Conversely, during CHF, the subgroup with high sympathetic activity had a high QTVI due primarily to increased QT_v. This increased QTVI probably reflects the structural myocardial damage and chronic neurohumoral activation that characterizes CHF. Our findings in this experimental study provide direct evidence that neural activity and QTVI are correlated (at least during CHF) albeit possibly not causally related thus strengthening our previous observations in patients with CHF receiving sympathetic stimulation (5). The ANS, and especially sympathetic nerve modulation, therefore seem able to cause chronic myocardial repolarization lability ultimately leading to malignant ventricular arrhythmias through a mechanism involving trigger activity, or reentry, or both (20,21). The myocardial tendency to undergo similar mechanisms can be indirectly measured in vitro as an increase in transmural dispersion of repolarization (TDR), namely the maximum difference in the duration of the cardiac action potential between the various myocardial layers (20,21). An increased TDR induces the so-called discordant and concordant repolarization alternans (22–25), and this repolarization phenomenon depends on the prolonged M cell action potential (22). A marked action potential prolongation in M cells causing augmented TDR nevertheless becomes evident in abnormal conditions associated with increased arrhythmia susceptibility, such as congenital long QT syndrome but also CHF. Reduced I_{Ks}, however, amplifies TDR only in the presence of beta-adrenergic influence, due to a larger augmentation of residual I_{Ks} in epicardial and endocardial cells than in M cells. Indeed, sympathetic activity could be responsible for both the increased TDR and augmented QTVI, thus explaining why these 2 variables both correlate strictly with SCD (7–9,25–27).

In a recent study in healthy subjects, we observed that during sympathetic stimulation the duration of myocardial repolarization diminishes whereas the QTVI remains almost unchanged. Conversely, during CHF the QT interval lengthened, and the variables QT_v and QTVI increased (5). The mechanisms underlying the prolonged QT interval and QT_v during sympathetic activation in CHF remain unclear. Whereas some investigators attribute the CHF-induced QT changes to faulty regulation of Ca^{2+} cytosol channels (26), others invoke down-regulation of potassium channels (I_{to}, I_{Kr}, I_{Ks}, and I_{K1}) (27). During CHF, the mechanisms involving altered control of Ca^{2+} or K^+ channels might, however, operate together their contribution varying from individual to individual thus explaining prolonged myocardial repolarization.

Repolarization reserve and the ANS

The concept of repolarization reserve denotes functioning ion channel redundancy that can compensate for damaged channels if necessary (28). For example, a genetically weak I_{Ks} does not necessarily lead to overt long QT syndrome type 1 because a robust compensatory function of I_{Kr} maintains normal cardiac repolarization. Nevertheless in individuals with weak I_{Ks},

torsade de pointes can more easily be triggered during certain morbid conditions (including hypopotassemia, fever, myocardial ischemia, and CHF) or also after administration of I_{Kr} inhibitors (including d-sotalol, dofetilide, amiodarone, and macrolides) (28). Similarly, we conjecture that the prolonged QT interval we observed during sympathetic activation after pacing-induced CHF in the canine model used in this study arises through a mechanism that modulates Ca^{2+} and K^+ channel function, ultimately reducing repolarization reserve. A minor point to consider in interpreting our results is that rather than merely increasing sympathetic and reducing vagal activity, CHF induces wide fluctuations in QT duration (12). Hence, CHF might also lead to wide temporal fluctuations in repolarization reserve including times when sympathetic activity predominates characterized by a larger reduction in repolarization reserve and a greater predisposition to arrhythmic events (12) and safer times of vagal predominance.

Although others have already reported a prolonged QT during sympathetic activation in experimental models in vitro and during electrical stellate ganglion stimulation in vivo (14), to our knowledge our study is the first to provide direct evidence confirming this finding in an experimental model using live animals free to move, and most important, without pharmacological interference.

Cross-spectral analysis of RR and QT intervals

Cross-spectral analysis was introduced by Berger et al. (4) in the first study on QTVI designed to show that RR interval and QT variables agreed. Coherence is measured as the R correlation factor: a high spectral coherence value is near 1, a low spectral coherence value is close to 0. Albeit controversial (29), a coherence value of less than 0.500 is arbitrarily considered to reflect low coupling, especially for certain cardiovascular signals (i.e., between heart rate and blood pressure) (30–32). In their original study, Berger et al. (4) reported relatively low spectral coherence between RR and QT (<0.500) and later studies confirmed this low value also in healthy subjects (6,33,34) and in patients with CHF (6,33,34). In our study, conducted in a canine model of CHF, we achieved extraordinarily high spectral coherence values, almost twice as high as those reported in studies in humans.

This elevated QT-RR coherence suggests that the 2 signals vary in parallel and that our recording technique yields a qualitatively excellent, noise-free QT signal (noise having a stochastic distribution). Some investigators question the template method of studying the QT (11), underlining that this technique yields recordings with high noise levels. Hence, under our experimental conditions, the QT template method seems an excellent technique. Although we cannot explain why the canine model yields such high spectral coherence, a possible reason is that ECG signals recorded from dogs remain uninfluenced by skin impedance because the recording electrodes are implanted subcutaneously. An alternative explanation is that recording electrode montages differ in humans and dogs. Whereas in humans recording electrodes are placed according to a standard montage (leads II or III), in dogs they are placed in the best site for exploring the electrical field crossed by the major depolarization vector in the left ventricle (1 electrode is positioned proximally and anteriorly to the left hemithorax and the other posteriorly and distally in a lower position). Last, we cannot exclude the possibility that canine Ca^{2+} and K^+ channels might be more sensitive to ANS activity than the corresponding channels in human myocardium.

Further support for the close relationships between the ANS and temporal myocardial repolarization dispersion came from our finding that at baseline QT-RR coherence values were higher in the subgroup with high sympathetic activity values than in those recorded at low values, whereas during CHF we found no difference between the 2 subgroups (Fig. 6), but QT_v and the QTVI (indexes of temporal myocardial repolarization dispersion) increased. The increased QT_v during CHF during high sympathetic activity leads to temporal QT-RR interval coherence (4). The increased coherence at baseline in segments recorded at high sympathetic

activity values was a partially unexpected finding. One explanation for this phenomenon is that in mammals I_{Ks} channels normally take no more than a minor part in cardiac repolarization under conditions of normal heart rate (35–37), whereas I_{Kr} channels play a major role (37). When adrenergic stimulation causes the heart rate to increase, then I_{Ks} channels act to adapt repolarization: the shorter the cycle length the greater the need for rapid repolarization and recruitment of all available potassium channels (36,37). From this viewpoint, the increased QT-RR interval coherence we observed under healthy conditions could be interpreted as a marker of adequate I_{Ks} channel recruitment, whereas during CHF I_{Ks} channels being down-regulated, the foregoing mechanisms function inadequately, and QT-RR coherence remains constant even though QT_v and, hence, QTVI increase.

Study limitations

In this study we recorded ANS activity from the vagal nerve and left stellate ganglion because these nerves exert the major direct influence on cardiac repolarization (14,38). Although RR interval variability is influenced above all by right sympathovagal innervation to the sinus node, unfortunately the DSI we used comprises only 3 recording channels and we especially sought detailed information on cardiac repolarization. Nevertheless, we have already shown in a previous study a good correlation between right and left sympathetic activity a single recording channel probably suffices to guarantee the knowledge of global sympathetic innervation (39) in dogs.

A second limitation of the study is that although all the segments analyzed were obtained within the first week after inducing CHF, we discarded those obtained immediately after turning the pacemaker off. We did so because they contain innumerable arrhythmias, whereas study protocols designed to investigate heart rate or QT variability require at least 256 consecutive beats in sinus rhythm. The chosen timing probably has the disadvantage of excluding epochs recorded during maximal sympathetic activity and allowing dogs slight vagal recovery (40).

A third limitation is that rather than assessing eventual changes in myocardial repolarization close to an acute event, our study assesses electrical remodeling during CHF. As did Berger et al. (4) in their first report, we merely observed that CHF is associated with increased sympathetic activity and increased temporal dispersion in myocardial repolarization, conditions that favor the onset of malignant ventricular arrhythmias.

Another limitation is that we have no information on the type of activity or the dog's position when data were recorded. Yet, insofar as QT analysis requires noise-free recordings, our data most probably refer to dogs at rest. From a point of view of ANS, what matters most is not what the dog was doing when the data were recorded but the changes associated with the activity. In other words, regardless of whether dogs were asleep or awake, the scope of our study was not to assess which of the 2 conditions induces major sympathetic activation but to find out whether major sympathetic activation is associated with altered myocardial repolarization under normal conditions and during CHF.

Last, the heart rate we recorded in ambulatory dogs at given levels of sympathetic activity and vagal control was lower before than during CHF (Table 1). This finding might easily be explained by the fact that during CHF the larger amounts of surrenal circulating epinephrine could stimulate cardiac beta-receptors and maintain a higher heart rate, but to prove this mechanism we would need to study cardiac catecholamine spillover. Another more speculative explanation is that if levels of 1 neurotransmitter decline then the other maintains heart rate levels high although adrenaline alone is unable to shorten the duration of cardiac repolarization. Finally, the increased heart rate we observed during CHF might depend on sinus dysfunction and electrical remodeling (41).

Conclusions

Whereas our study shows an association between augmented sympathetic activity and the increased QTVI during CHF, it provides no evidence of a similar association under normal conditions. The findings obtained in this CHF canine model suggest that the QTVI—an index closely related to the risk of SCD (7–9)—could also be used as a reliable marker of neurohumoral activation and, hence, of disease progression.

Acknowledgments

Abbreviations and Acronyms

ANS
 autonomic nervous system

CHF
 congestive heart failure

DSI
 Data Sciences International

iSGNA
 integrated left stellate-ganglion nervous activity

iVNA
 integrate vagus nerve activity

QTc
 corrected QT interval

QT$_m$
 QT mean

QT$_v$
 QT variance

QTVI
 QT variability index

RR$_m$
 RR mean

RR$_v$
 RR variance

SCD
 sudden cardiac death

TDR
 transmural dispersion of repolarization

References

1. Zipes DP, Wellens HJ. Sudden cardiac death. Circulation 1998;98:2334–51. [PubMed: 9826323]

2. Tomaselli GF, Zipes DP. What causes sudden death in heart failure? Circ Res 2004;95:754–63. [PubMed: 15486322]

3. Jin H, Lyon AR, Akar FG. Arrhythmias mechanisms in the failing heart. Pacing Clin Electrophysiol 2008;31:1048–56. [PubMed: 18684263]

4. Berger RD, Kasper EK, Baughman KL, et al. Beat-to-beat QT interval variability. Novel evidence for repolarization lability in ischemic and nonischemic dilated cardiomyopathy. Circulation 1997;96:1557–65. [PubMed: 9315547]

5. Piccirillo G, Magnanti M, Matera S, et al. Age and QT variability index during free breathing, controlled breathing and tilt in patients with chronic heart failure and healthy control subjects. Transl Res 2006;148:72–8. [PubMed: 16890147]

6. Piccirillo G, Quaglione R, Nocco M, et al. Effect of long-term beta-blocker (metoprolol or carvedilol) therapy on QT variability in subjects with chronic heart failure secondary to ischemic cardiomyopathy. Am J Cardiol 2002;90:113–7.

7. Atiga WL, Calkins H, Lawrence JH, Tomaselli GF, Smith JM, Berger RD. Beat-to-beat repolarization lability identifies patients at risk for sudden cardiac death. J Cardiovasc Electrophysiol 1998;9:899–908. [PubMed: 9786070]

8. Haigney MC, Zareba W, Gentlesk PJ, et al. QT interval variability and spontaneous ventricular tachycardia or fibrillation in the Multi-center Automatic Defibrillator Implantation Trial (MADIT) II. J Am Coll Cardiol 2004;44:1481–7. [PubMed: 15464332]

9. Piccirillo G, Magrì D, Matera S, et al. QT variability strongly predicts sudden cardiac death in asymptomatic subjects with mild or moderate left ventricular systolic dysfunction: a prospective study. Eur Heart J 2007;28:1344–50. [PubMed: 17101636]

10. Baumert M, Lambert GW, Dawood T, et al. QT variability index during rest not correlated with cardiac spillover in patients with depression and panic disorders. Am J Physiol Heart Circ Physiol 2008;295:H962–8. [PubMed: 18599596]

11. Malik M. Beat-to-beat QT variability and cardiac autonomic regulation. Am J Physiol Heart Circ Physiol 2008;295:H923–5. [PubMed: 18641269]

12. Ogawa M, Zhou S, Tan AY, et al. Left stellate ganglion and vagal nerve activity and cardiac arrhythmias in ambulatory dogs with pacing-induced congestive heart failure. J Am Coll Cardiol 2007;50:335–43. [PubMed: 17659201]

13. Tan AY, Zhou S, Ogawa M, et al. Neural mechanisms of paroxysmal atrial fibrillation and paroxysmal atrial tachycardia in ambulatory canines. Circulation 2008;118:916–25. [PubMed: 18697820]

14. Zhou S, Jung BC, Tan AY, et al. Spontaneous stellate ganglion nerve activity and ventricular arrhythmias in a canine model of sudden death. Heart Rhythm 2008;5:131–9. [PubMed: 18055272]

15. Okuyama Y, Miyauchi Y, Park AM, et al. High resolution mapping of the pulmonary vein and the vein of Marshall during induced atrial fibrillation and atrial tachycardia in a canine model of pacing-induced congestive heart failure. J Am Coll Cardiol 2003;42:348–60. [PubMed: 12875775]

16. Benitez D, Gaydecky PA, Zaidi A, Fitzpatrick AP. The use of the Hilbert transform in ECG signal analysis. Comput Biol Med 2001;31:399–406. [PubMed: 11535204]

17. Task Force of the European Society of Cardiology and the North American Society of Pacing and Electrophysiology. Heart rate variability. Standard of measurements, physiological interpretation and clinical use. Circulation 1996;93:1043–65. [PubMed: 8598068]

18. Tabo M, Nakamura M, Kimura K, Ito S. QT-RR relationship and suitable QT correction formulas for halothane-anesthetized dogs. J Toxicol Sci 2006;31:381–90. [PubMed: 17077591]

19. Hirimoto K, Shimizo H, Mine T, Masuyama T, Ohyanagy M. Correlation between beat-to-beat QT interval variability and impaired left ventricular function in patients with previous myocardial infarction. Ann Noninvasive Electrocardiol 2006;11:299–305. [PubMed: 17040277]

20. Antzelevitch C. Heterogeneity and cardiac arrhythmias: an overview. Heart Rhythm 2007;4:964–72. [PubMed: 17599687]

21. Li G-R, Feng J, Yue L, Carrier M. Transmural heterogeneity of action potential and I_{to1} in myocytes isolated from the human right ventricle. Am J Physiol 1998;275:H369–77. [PubMed: 9683422]

22. Akar FG, Rosenbaum DS. Transmural electrophysiological heterogeneities underlying arrhythmogenesis in heart failure. Cir Res 2003;93:638–45.

23. Pastore JM, Girouad SD, Laurita KR, Akar FG, Rosenbaum DS. Mechanism linking T-wave alternans to the genesis of cardiac fibrillation. Circulation 1999;99:1385–94. [PubMed: 10077525]

24. Koller ML, Riccio ML, Gilmour RF. Dynamic restitution of action potential duration during electrical alternans and ventricular fibrillation. Am J Physiol 1998;44:H1635–42. [PubMed: 9815071]

25. Rosen MR, Cohen IS. Molecular/genetic determinants of repolarization and their modification by environmental stress. J Int Med 2006;259:7–23.

26. Jin H, Lyon RA, Akar F. Arrhythmia mechanisms in the failing heart. Pacing Clin Electrophysiol 2008;31:1048–56. [PubMed: 18684263]

27. Tomaselli GF, Zipes DP. What causes sudden death in heart failure? Circ Res 2004;95:754–63. [PubMed: 15486322]

28. Roden DM. Long QT syndrome: reduced repolarization reserve and genetic link. J Int Med 2006;259:59–69.

29. Robbe HWJ, Mulder LJM, Rüddel H, Langewitz WA, Veldman JBP, Mulder G. Assessment of baroreceptor reflex sensitivity by means of spectral analysis. Hypertension 1987;10:538–43. [PubMed: 3666866]

30. Pagani M, Somers V, Furlan R, et al. Changes in autonomic regulation induced by physical training in mild hypertension. Hypertension 1988;12:600–10. [PubMed: 3203964]

31. Pitzalis MV, Mastropasqua F, Passantino A, et al. Comparison between noninvasive indices of baroreceptor sensitivity and the phenylephrine method in post myocardial infarction patients. Circulation 1998;97:1362–7. [PubMed: 9577947]

32. Pinna GD, Meastri R. New criteria for estimating baroreflex using the transfer function method. Med Biol Eng Comput 2002;40:79–84. [PubMed: 11954712]

33. Piccirillo G, Cacciafesta M, Lionetti M, et al. The influence of age, the autonomic nervous system and anxiety on QT interval variability. Cli Sci 2001;101:429–38.

34. Piccirillo G, Germanò G, Quaglione R, et al. QT interval and autonomic control in hypertensive subjects with left ventricular hypertrophy. Clin Sci 2002;102:363–71. [PubMed: 11869178]

35. Shimizu W, Antzelevitch C. Differential effects of beta-adrenergic agonists and antagonists in LQTS1, LQTS2 and LQTS3 models of the QT syndrome. J Am Coll Cardiol 2000;35:778–86. [PubMed: 10716483]

36. Volders PGA, Stengl M, van Opstal JM, et al. Probing the contribution of I_{Ks} to canine ventricular repolarization. Kay role for β-adrenergic receptor stimulation. Circulation 2003;107:2753–60. [PubMed: 12756150]

37. Jost N, Virag L, Bitay M, et al. Restricting exercise cardiac action potential and QT prolongation: a vital role for I_{Ks} in human ventricular muscle. Circulation 2005;112:1392–9. [PubMed: 16129791]

38. Schwartz PJ, Stone HL. Left stellectomy in prevention of ventricular fibrillation caused by acute myocardial ischemia in conscious dogs with anterior myocardial infarction. Circulation 1980;62:1256–65. [PubMed: 7438361]

39. Joung BC, Dave AS, Tan AY, et al. Circadian variation of stellate ganglion nerve activity in ambulatory dogs. Heart Rhythm 2006;3:78 – 85. [PubMed: 16399059]

40. Motte S, Mathieu M, Brimioulle S, et al. Respiratory-related heart variability in progressive experimental heart failure. Am J Physiol Heart Circ Physiol 2005;289:H1729–35. [PubMed: 15923309]

41. Sanders P, Kistler PM, Morton JB, Spence SJ, Kalman JM. Remodeling of sinus-node function in patients with congestive heart failure: reduction in sinus-node reserve. Circulation 2004;110:897–903. [PubMed: 15302799]
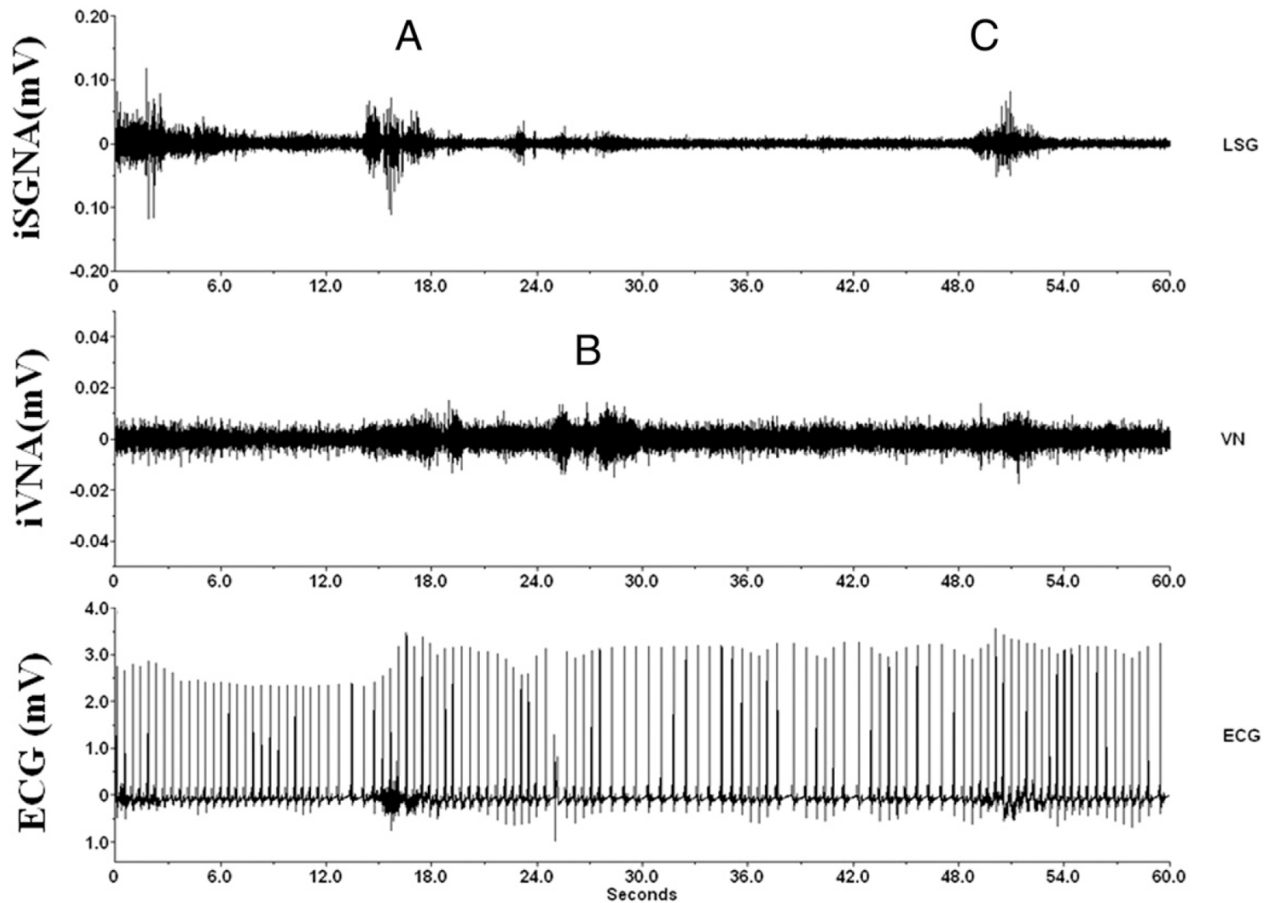
Figure 1. Nerve and ECG Recordings
Example of simultaneous integrated stellate ganglion nerve activity (iSGNA) and integrated
vagal nerve activity (iVNA) at baseline (before pacing-induced congestive heart failure) in an
ambulatory dog. **(Top)** iSGNA; **(middle)** iVNA; **(bottom)** electrocardiographic (ECG) trace.
In the upper trace, **A** indicates between the 12th and 16th s, an epoch of high sympathetic
activity followed 3 s later by an epoch of fast heart rate (about 120 beats/min, between the 18th
and 24th s). This sympathetic activity is followed almost immediately, between the 24th and
30th s, by a vagal increase with lower heart rate **(B)** (from 120 to 90 beats/min, between the
30th and 36th s), and last **(C)**, a new increase in sympathetic activity after the 48th s, and a
heart rate increase (from 90 to 130 beats/min, around the 54th s). LSG = left stellate ganglion
nerve; VN = vagal nerve.
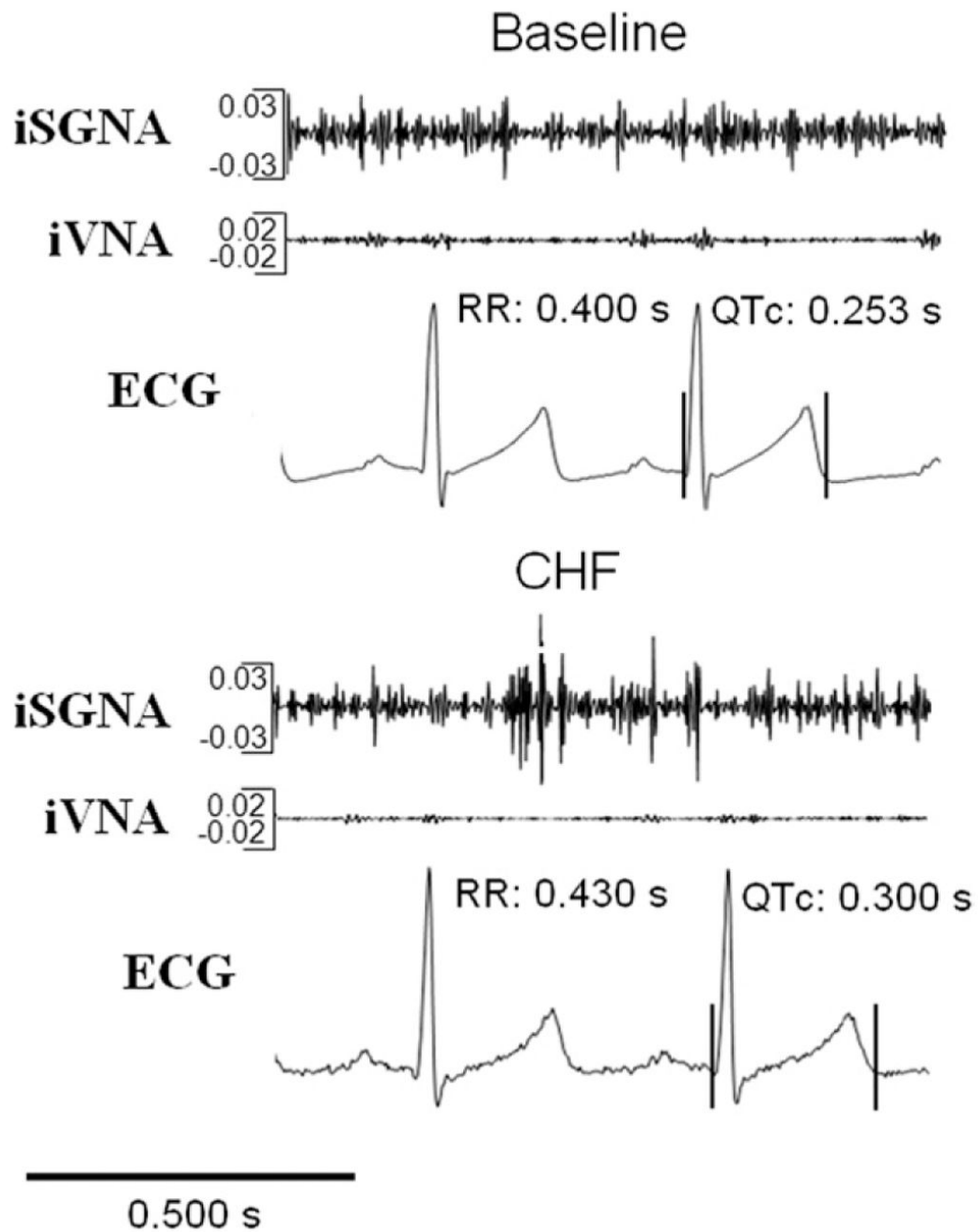
Figure 2. Integrate Nerve Recordings and QT Interval
Example of assessment of iSGNA, iVNA, and its influence on RR and QT intervals at baseline and after pacing-induced congestive heart failure (CHF) in an ambulatory dog. QTc = corrected QT interval; other abbreviations as in Figure 1.
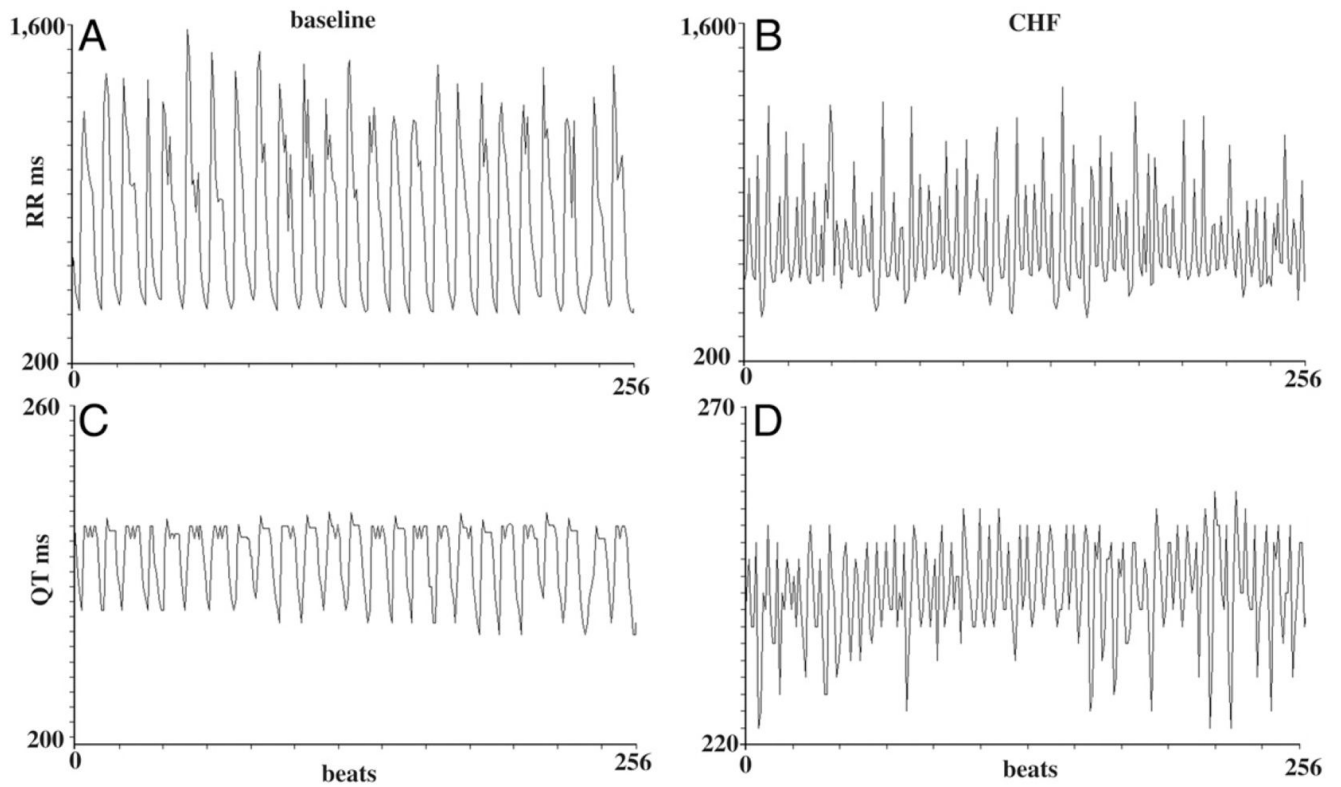
Figure 3. RR and QT Intervals in 256 Beats
RR and QT intervals recorded in the same dog at baseline (**A and C**) and during congestive heart failure (CHF) (**B and D**) under the same sympathetic activity levels. **A and C** show the RR recorded and QT intervals over 256 consecutive cycles at baseline, and **B and D** show the same data during CHF.
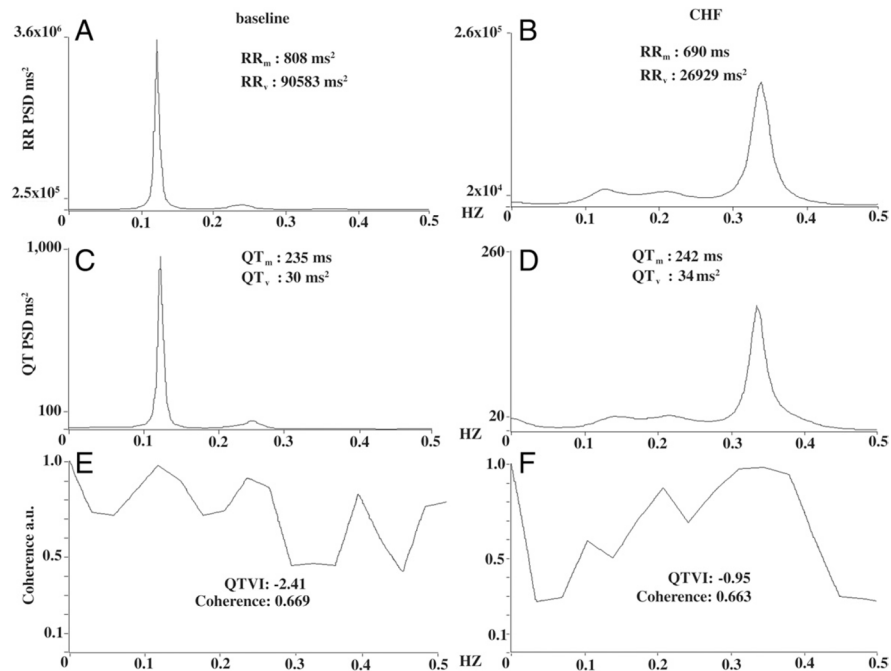
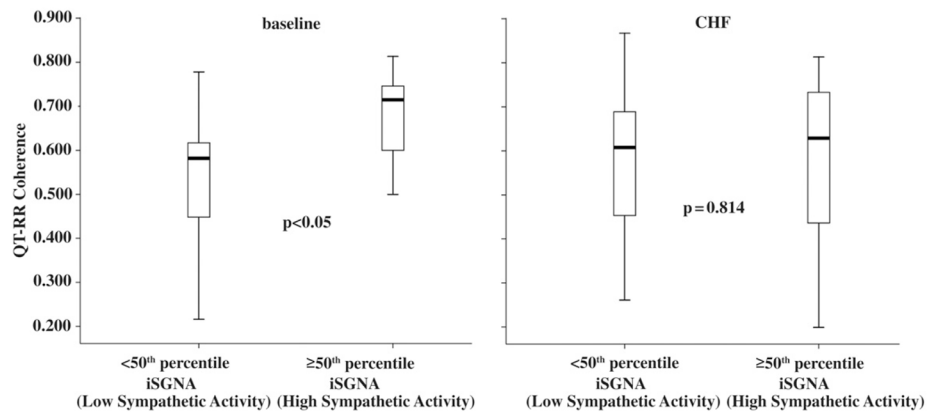**Figure 4. Power Spectral Analysis, Coherence, and QTVI**

RR and QT spectra obtained from the recordings of Figure 3. As in Figure 3, we reported the spectrum in the same dog at baseline **(left panels)** and during congestive heart failure (CHF) **(right panels)** under the same sympathetic activity levels. **Panel A** shows the power spectra for RR intervals at baseline, **panel B** during CHF. Note the dramatic reduction in RR-interval variance (RR_v), less than two-thirds the value during CHF, and the reduced RR interval (RR_m). **Panels C and D** show the spectra for QT intervals recorded at baseline and during CHF. Note that QT variance (QT_v) and the mean QT interval (QT_m) both increase. Last, **panels E** (baseline) **and F** (CHF) give coherence and corresponding QT variability index (QTVI) values calculated from the respective RR (baseline: **A**; CHF: **B**) and QT intervals (baseline: **C**; CHF: **D**) (QTVI = QTv/[QTm]2/RRv/[RRm]2). Note the increased QTVI during CHF. Note also that maximum coherence at baseline peaks at around 0.1 Hz and during in CHF at around 0.35 Hz. The maximum peak differs because the 2 synchronous spectral components RR **(A)** and QT **(C)** predominantly oscillate at a lower frequency at baseline than during CHF (0.1 and 0.35 Hz) **(B and D)**. PSD = power spectral density in the area under the curve.
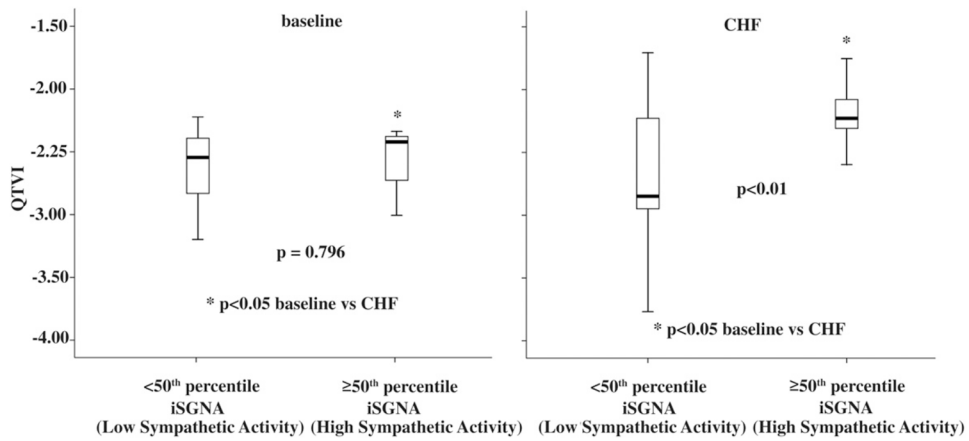
Figure 5. QTVI Changes in Baseline and in CHF
In the subgroup recorded at high sympathetic activity values, the QTVI was significantly lower at baseline than during CHF. In the **box plots**, the **central line** represents the median distribution. Each box spans from 25th to 75th percentile points, and **error bars** extend from 10th to 90th percentile points. iSGNA = integrated stellate ganglion nerve activity; other abbreviations as in Figure 4.

Figure 6. QT-RR Coherence Changes Between Baseline and CHF
Graph showing cross-spectral analysis (coherence) in the 6 ambulatory dogs. Note that baseline coherence increases as a function of the increase in spectral sympathetic nerve activity. In the **box plots**, the **central line** represents the median distribution. Each box spans from 25th to 75th percentile points, and **error bars** extend from 10th to 90th percentile points. CHF = congestive heart failure; iSGNA = integrated stellate ganglion nerve activity.

Table 1

QT and RR Variables Grouped for Low and High Sympathetic Activity at Baseline and After Pacing-Induced CHF

Variables	Baseline			CHF		
	Low Sympathetic Activity (<50th Percentile of iSGNA) (n = 18)		High Sympathetic Activity (≥50th Percentile of iSGNA) (n = 18)	Low Sympathetic Activity (<50th Percentile of iSGNA) (n = 18)		High Sympathetic Activity (≥50th Percentile of iSGNA) (n = 18)
RR_m, s	0.995 ± 0.300*	<0.001	0.696 ± 0.071	0.795 ± 0.120	0.104	0.727 ± 0.109
RR_v, ms^2	120,444 (369,936)*	<0.05	62,000 (14,844)*	45,004 (26,511)	<0.05	40,845 (15,110)
QT_m, s	0.291 ± 0.107	<0.001	0.218 ± 0.013†	0.231 ± 0.013	<0.05	0.241 ± 0.009
QT_v, ms^2	38 (56)	0.798	35 (21)	28 (10)	<0.001	61 (12)
QTc_{Bazett}	0.290 ± 0.053	0.162	0.262 ± 0.012†	0.260 ± 0.013	<0.001	0.283 ± 0.014
$QTc_{Fridericia}$	0.289 ± 0.069	0.098	0.246 ± 0.010†	0.250 ± 0.009	<0.001	0.268 ± 0.012
QTc_{Tabo}	0.289 ± 0.063	0.112	0.252 ± 0.011†	0.253 ± 0.010	<0.001	0.273 ± 0.012
$QTc_{Van de Water}$	0.292 ± 0.075	0.165	0.245 ± 0.010†	0.249 ± 0.009	<0.001	0.265 ± 0.009
$QTc_{Framingham}$	0.292 ± 0.053	0.089	0.265 ± 0.010†	0.262 ± 0.013	<0.001	0.283 ± 0.011
300 s iSGNA, mV	53 ± 21	<0.0001	140 ± 49	57 ± 13	<0.0001	147 ± 57
300 s iVNA, mV	45 ± 18	0.463	33 ± 12	40 ± 10	0.865	39 ± 19

*
p<0.05 baseline versus congestive heart failure (CHF);

†
p < 0.001 baseline versus CHF. **Bold** values indicate a statistical significance.

iSGNA = integrated stellate ganglion nerve activity; iVNA = integrated vagal nerve activity; QTc = corrected QT interval; QT_m = mean QT interval; QT_v = QT variance; RR_m = reduced RR interval; RR_v = RR-interval variance.

Table 2

Multiple Regression Analysis Between Direct Sympathetic Nerve Activity and QT Data at Baseline

	R	R^2	p Value	In 300 s iSGNA				In 300 s iVNA				Intercept		
				β	SE	Beta	p Value	β	SE	Beta	p Value	β	SE	p Value
RR$_m$, ms	0.61	0.37	**0.0001**	—	—	—	0.065	0.50	0.11	0.61	**0.0001**	−0.94	0.40	**0.025**
RR$_v$, ln ms^2	−0.62	0.39	**0.0001**	−0.62	0.27	30.50	0.001	0.78	0.28	0.37	**0.010**	11.4	1.3	**0.0001**
QT$_m$, ms	0.60	0.36	**0.0001**	—	—	—	0.160	0.13	0.03	0.60	**0.0001**	—	—	0.065
QT$_v$ ln ms^2	—	—	0.688	—	—	—	0.807	—	—	—	0.412	—	—	0.230
QTc$_{Bazett}$	0.49	0.24	**0.003**	—	—	—	0.421	0.05	0.02	0.48	**0.003**	—	—	0.083
QTc$_{Fridericia}$	0.56	0.31	**0.0001**	—	—	—	0.263	0.08	0.02	0.56	**0.0001**	—	—	0.944
QTc$_{Tabo}$	0.54	0.29	**0.001**	—	—	—	0.302	0.07	0.02	0.54	**0.001**	—	—	0.644
QTc$_{Van de Water}$	0.57	0.32	**0.0001**	—	—	—	0.256	0.08	0.02	0.57	**0.0001**	—	—	0.661
QTc$_{Framingham}$	0.50	0.25	**0.002**	—	—	—	0.503	0.05	0.01	0.50	**0.002**	—	—	0.081
QTVI	0.40	0.16	**0.012**	—	—	—	0.460	30.47	0.17	30.41	**0.012**	—	—	0.204

Bold values indicate a statistical significance.

Abbreviations as in Table 1.

Table 3

Multiple Regression Analysis Between Direct Sympathetic Nerve Activity and QT Data After Pacing-Induced CHF

	R	R^2	p Value	ln 300 s iSGNA				ln 300 s iVNA				Intercept		
				β	SE	Beta	p Value	β	SE	Beta	p Value	β	SE	p Value
RR_m, ms	—	—	0.106	—	—	—	0.119	—	—	—	0.106	—	—	0.090
RR_v, ln ms^2	—	—	0.073	—	—	—	0.642	—	—	—	0.095	—	—	0.056
QT_m, ms	0.42	0.18	**0.010**	0.010	0.004	0.42	**0.010**	—	—	—	0.320	0.19	0.02	**0.0001**
QT_v ln ms^2	0.49	0.24	**0.002**	0.008	0.003	0.49	**0.002**	—	—	—	0.940	1.9	0.30	**0.0001**
QTc_{Bazett}	0.55	0.30	**0.0001**	0.018	0.005	0.55	**0.001**	—	—	—	0.503	0.19	0.02	**0.0001**
$QTc_{Fridericia}$	0.59	0.35	**0.0001**	0.015	0.003	0.59	**0.0001**	—	—	—	0.482	0.19	0.01	**0.0001**
QTc_{Tabo}	0.58	0.34	**0.0001**	0.016	0.004	0.58	**0.0001**	—	—	—	0.466	0.19	0.02	**0.0001**
$QTc_{Van de Water}$	0.59	0.35	**0.0001**	0.013	0.003	0.59	**0.0001**	—	—	—	0.450	0.20	0.01	**0.0001**
$QTc_{Framingham}$	0.54	0.30	**0.0001**	0.016	0.005	0.52	**0.0001**	—	—	—	0.489	0.20	0.02	**0.0001**
QTVI	0.57	0.32	**0.010**	0.27	0.13	0.34	**0.01**	—	—	—	0.308	33.6	0.60	**0.0001**

Bold values indicate a statistical significance.

QTVI = QT variability index; other abbreviations as in Table 1.